ARTICLES

Interaction and energy transfer between divalent Sm ions and CN^- molecular defects in KCl

V. Dierolf
Fachbereich Physik, Universität-GH, D-33095 Paderborn, Germany
(Received 13 April 1999)

We studied the mutual interaction and electronic-vibrational energy transfer processes between divalent samarium ions and neighboring CN^- molecular impurities in KCl by the highly site-selective technique of combined excitation-emission spectroscopy as well as by vibrational CN^- luminescence (VL). We found for Sm^{2+}-CN^- complexes involving just a single CN^- molecule that the spectral shifts of the intraconfigurational ($4f \leftrightarrow 4f$) transitions are very small, and are about 10 times bigger for the interconfigurational ($4f^6 \leftrightarrow 4f^5 5d^1$) transitions. No measurable energy transfer from the electronic excitation into the vibrational CN^- stretch mode takes place for those centers, reflecting the weakly interacting character of the energetically lowest excited $^5D_0$ state which belongs to the $4f$-electronic configuration. However, for more complex centers which appear for higher CN^- concentrations and involve more than one CN^- molecule the more strongly coupled $5d$-type states are shifted to lower energy, even below the $^5D_0$ state. In this case E-V energy transfer can be observed by the appearance of VL. [S0163-1829(99)07941-2]

I. INTRODUCTION AND BACKGROUND

In the recent past, the interaction and the electronic-vibrational (E-V) energy transfer processes between an electronic and a molecular defect have been studied experimentally in various systems[1–11] and several theoretical models for interpretation have been proposed.[12–16] The main focus in these investigations was on those combinations of defects [F-center–CN^-, F-center–OH^-, Yb^{2+}-$(CN^-)_n$], which exhibit strong mutual coupling effects. Common to all these systems is a relatively strong electron-phonon coupling of the relevant electronic defect states which is reflected in the corresponding Hyang-Rhys factor S (e.g., $S=10$–100 for F centers). This apparent connection between the coupling to the vibrational modes of the lattice and to those of the neighboring molecular defect has not been investigated experimentally in detail. Especially, electronic states, which are only weakly influenced by the surrounding ions, have not been considered. Possible candidates for such investigations could be the trivalent rare earth ions with their transitions between well shielded $4f$ states which have been used as laser-active ions for various applications. Unfortunately, it is in general not possible to introduce those ions into alkali halides in which all the mentioned studies have been carried out. As an alternative, divalent rare earth ions, like Eu^{2+} and Sm^{2+}, may be used which can be incorporated quite easily and have been well characterized already as individual defects.[17] While the $4f \rightarrow 4f$ transitions of Eu^{2+} with CN^- neighbors have been studied by two-photon absorption,[18] revealing essentially no interaction effect, we chose for our investigation the Sm^{2+} ion for which the electronic transition both among $4f$ states (intraconfigurational) as well as between $4f$ and $5d$ states (interconfigurational) can be observed in absorption and emission in the visible spectral region, allowing a direct comparison.

The excitation-relaxation cycle of an isolated Sm^{2+} defect in KCl, consisting of the Sm^{2+} ion and a charge compensating vacancy as its $\langle 110 \rangle$ neighbor,[19,20] is illustrated in Fig. 1 using schematic energy level diagrams proposed by Guzzi and Baldini.[21] After excitation into the $5d$-type excited state and rapid relaxation into the ($4f$-type) $^5D_0$ state, transitions into the ^7F_j states take place, giving rise to a spectrum which at low temperatures ($T<15$ K) consists of seven groups of sharp lines stretching from the visible into the near infrared. Due to the $4f \leftrightarrow 4f$ character of the transition, the lifetime is quite long (≈ 10 ms). For higher temperatures a broad emission background with a much higher decay rate appears, indicating a thermally activated population of a $5d$-type state (E) which lies only slightly (0.016 eV for KCl)

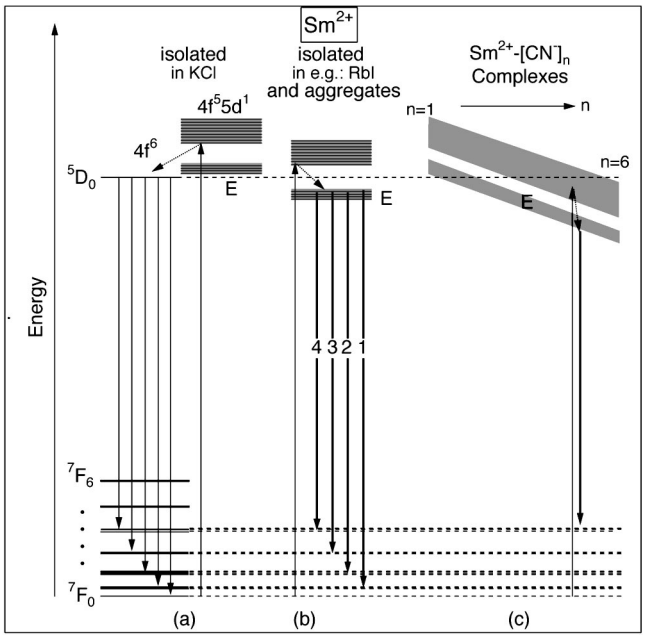

FIG. 1. Schematic energy level diagram for the lowest states of (a) isolated Sm^{2+} in KCl, (b) isolated Sm^{2+} in, e.g., RbI and Sm^{2+} aggregates in KCl, and (c) Sm^{2+}-$(CN^-)_n$ complexes in KCl.

above. Due to its $5d$ character, this level is fairly sensitive to changes in the host material and it lies, e.g., for RbI, KI, NaCl, NaBr, NaI, and CaF_2,[17,21] even below the ^5D_o state [Fig. 1(b)]. Under these conditions the emission properties are altered: The luminescence is spectrally much broader and has already at low temperatures a much shorter radiative lifetime as well as a high quantum efficiency. These features have been used successfully in the CaF_2 host material for the realization of a solid state laser.[22]

The electron-phonon interaction of the Sm^{2+} in KCl was experimentally studied by Baldini and Guzzi[23] as well as by Bron and Heller[20] who found a significant difference in the strength and spectral shape of the vibrational sidebands. These observations were explained by the difference in the nature of the coupling:[24] While the $4f \leftrightarrow 4f$ transitions exert only long-range forces causing exclusively (although weak $S \approx 1$) interaction with unperturbed crystal phonons, the $4f \leftrightarrow 5d$ transitions involve also short-range force contributions, causing an interaction with local (impurity-related) phonon modes ($S \approx 5$).

Among possible molecular partners for the Sm^{2+} we selected CN^- because for this molecule the vibrational transitions are at least partially radiative which allows us to study the energy transfer by vibrational luminescence spectroscopy around 5 μm. The described properties make the Sm^{2+}-$(CN^-)_n$ complex system an interesting model case to investigate the following questions.

(1) Regarding the spectral position and electron-phonon coupling, how are the different types of Sm^{2+} states influenced by the presence of CN^- neighbors?

(2) Can E-V energy transfer originating from the well-shielded $4f$ states take place and how is the process altered when the more strongly electron-phonon coupled $5d$ states are involved?

Starting with the description of the sample preparation, the main experimental techniques (Sec. II), and the presentation of the experimental results (Sec. III), these questions will be discussed in the final section (Sec. IV).

II. EXPERIMENTAL TECHNIQUES

The samples we used in this study were grown in the Paderborn crystal growth facility by the Bridgman technique. All samples were nominally doped with 0.1% of Sm^{2+} by adding $SmCl_2$ to the melt. The various concentrations of the CN^- codopant were determined by absorption measurements in the infrared. For comparison several samples from the crystal growth laboratory at the University of Utah were employed. In order to achieve a statistical distribution of all the defects and to keep the number of $[Sm^{2+}]_n$ aggregates at a minimum[19] we rapidly quenched the sample from 600 °C before we mounted it into a He-flow cryostat and cooled it to $T=10$ K. The expected (and observed) spectral changes in the optical transitions of the Sm^{2+} induced by CN^- neighbors are very small. Moreover, the formed complexes have to be distinguished from $[Sm^{2+}]_n$ aggregates which are always present even in carefully quenched samples.[25] For these reasons we used the very selective combined excitation-emission spectroscopy (CEES) technique in which we recorded a large number (>200) of emission spectra at a dense sequence of excitation energies using a 0.85 m double monochromator (Spex 1402) and a optical multichannel analyzer (OMA, SI IRY700). The samples were excited by a tunable dye laser (Spectra Physics model 375, Ar^+-laser-pumped, DCM dye) with the wavelength controlled by a wavemeter (Burleigh WA2500 Jr.). The spectral resolution for both emission and excitation was better than 0.1 meV. The whole experimental setup was computer controlled to minimize the measuring time. The resulting two-dimensional (2D) data set of emission intensities as a function of emission and excitation wavelength $I(\lambda_{exc},\lambda_{em})$ or energy is best visualized using a contour plot in which lines of equal emission intensities are drawn. In such a representation, a single emission line excited in a single absorption transition appears—similar to a geographic map—as a mountain. This way the optical transitions of defects situated on different lattice sites or crystalline environments can be identified very clearly, as we will show below.

The vibrational luminescence spectra were recorded by conventional techniques using a LN-cooled InSb detector mounted behind a 0.25 m monochromator (Spex1675).

III. EXPERIMENTAL RESULTS

In this work we concentrated on measurements at low temperatures typically around $T=10$ K to achieve high selectivity and to avoid the complication of the emission spectra by the thermal activation mentioned above.

A. Isolated Sm^{2+} defects

The absorption, excitation, and emission spectra of Sm^{2+} in KCl have been already studied in much detail[19] and are in most aspects reproduced by our own investigations, thus giving an excellent basis for our study. However, those earlier studies concentrated on very different aspects, so that we will present in the following some additional data relevant for this work. As a first example for the usefulness and sensitivity of the CEES technique and for comparison later on, we show in Fig. 2 the contour plot obtained from emission spectra for a KCl sample which has been doped only with Sm^{2+}. The spectral region shown was selected to include just a *single* peak for each center, i.e., the single $^7F_0 \rightarrow {}^5D_0$ transition in excitation and the line with highest energy out of the crystal field split $^5D_0 \rightarrow {}^7F_1$ transitions in emission. Hence each mountain which is found corresponds to a *different* center type. The strongest peaks are labeled *a* and *d* according to Ref. 19 where site *a* has been identified as the main site which consists of a Sm^{2+} with a charge compensating cation (K) vacancy as one of its next-nearest neighbors in the $\langle 110 \rangle$ direction. These two sites *a* and *d* can also be observed easily in individual emission and excitation spectra as shown in Figs. 2(b), and 2(c). A closer look at the combined spectrum reveals at least two more peaks. They are about two orders of magnitude weaker than the main peak. While one of them (d^*) can easily be obscured by the emission from site *d*, the other one (n) is well separated but is so weak that it was not among the reported ones (a-m) in Ref. 19.

The importance of the quenching procedure is reflected in the emission and excitation spectra for a KCl:Sm^{2+} sample

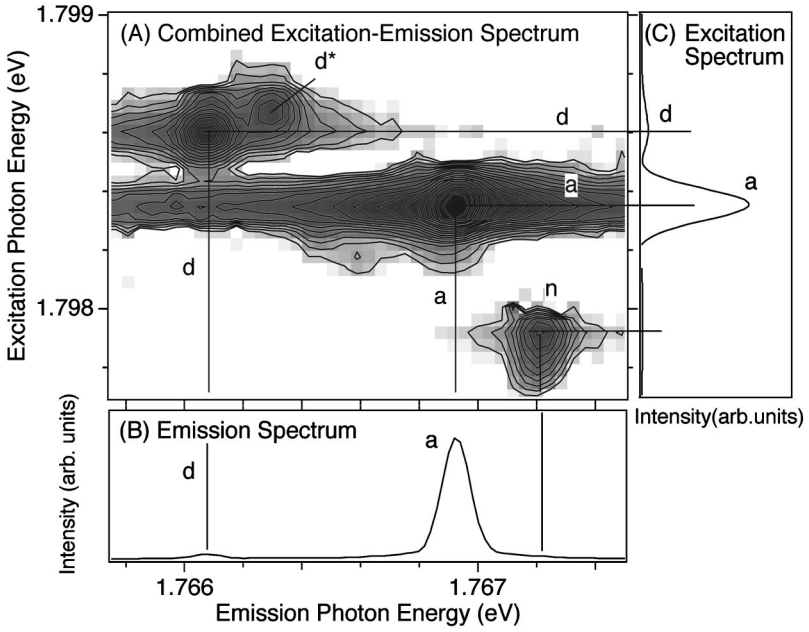

FIG. 2. Site-selective spectra of Sm^{2+} in KCl: (A) Combined-excitation-emission spectrum, (B) emission spectrum for a broadband excitation around 689 nm, and (C) excitation spectrum of emission probed with low spectral resolution (702 nm$\pm$2 nm). The different sites are labeled as in Ref. 19.

which has been stored several months in the dark at room temperature. Under these conditions a center aggregation can take place[25] which reveals itself by a drastically changed emission spectrum (Fig. 3, left) which can be observed for a wide range of excitation energies (Fig. 3, right) and which disappears after the sample is quenched. The emission consists of a broad background on top of which several groups (1, . . . ,4) of rather sharp lines are situated. These groups consist of lines separated by $\approx$11 meV. By further spectral expansion (see inset) it becomes obvious that the spectral lines have an additional substructure. In the excitation spectrum of the emission probed at around 1.55 eV (800 nm) we found also a broadband with a substructure between 1.90 eV (650 nm) and 1.85 eV (670 nm) consisting of one sharp and few less pronounced maxima which suggests a electron-phonon coupling similar as observed for transitions to $5d$-type states.

These and the published spectra for isolated Sm^{2+} and aggregated Sm^{2+} complexes can now be used and compared to the spectra we obtained in samples which have been codoped with Sm^{2+} and CN^-, allowing a reliable identification of Sm^{2+}-$(CN^-)_n$ related centers.

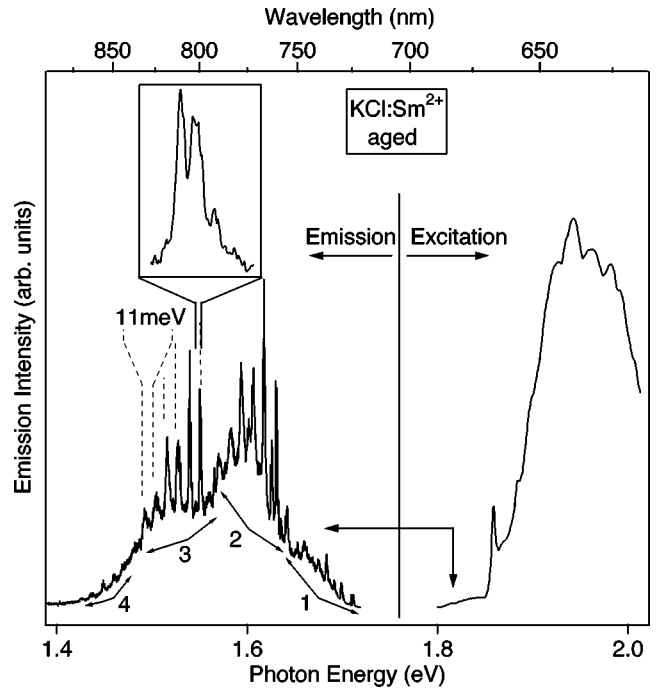

FIG. 3. Emission (left) and excitation (right) spectra of Sm^{2+} for a KCl sample which was stored for several weeks at room temperature. The emission was excited at the spectral position indicated by an arrow. Inset: substructure for the indicated emission line. The excitation spectrum was probed in the spectral range of the inset ($\approx$800 nm).

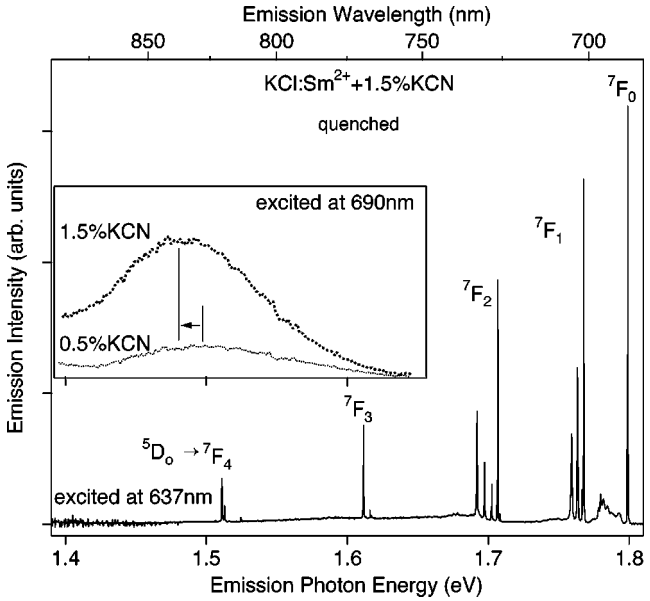

FIG. 4. Emission spectrum of Sm^{2+}-related defects in KCl:Sm^{2+} + 1.5% KCN excited at 637 nm. Inset: emission spectra excited at 690 nm for samples doped with 0.5% and 1.5% KCN. All samples were quenched from 600 °C just before the measurement.

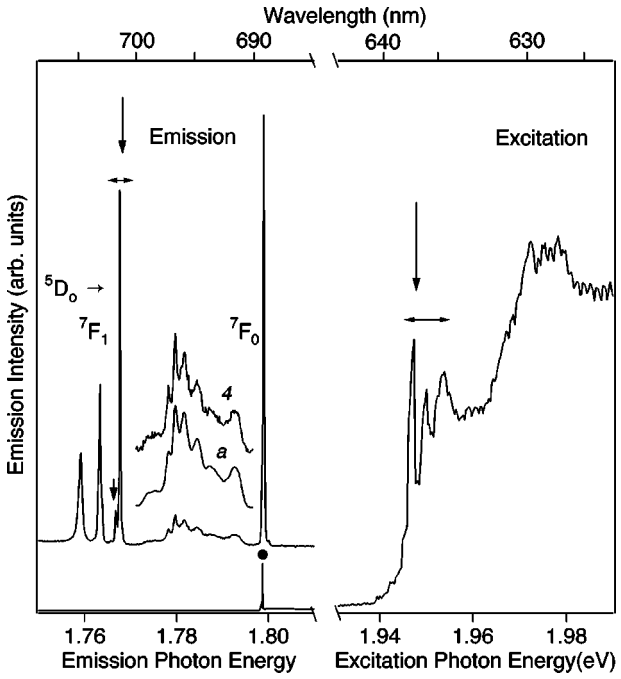

FIG. 5. Excitation and a more detailed emission spectra of Sm^{2+}-related defects in KCl:Sm^{2+} + 1.5% KCN excited at 637 nm. The sample was quenched from 600 °C just before the measurement. The position of probing and exciting the emission are indicated by vertical arrows. The vibrational sidebands of the $^5D_0 \leftrightarrow {}^7F_0$ transition are shown expanded for excitation of site *a* and 4 at 1.7984 eV and 1.7980 eV, respectively. The horizontal arrows and the point ● indicate the spectral ranges used in Fig. 6.

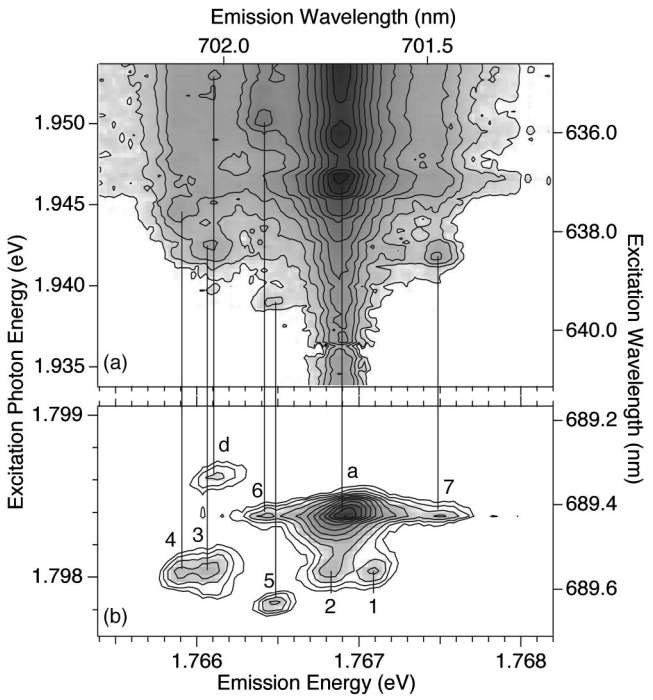

FIG. 6. Combined excitation-emission spectra of KCl:Sm^{2+} + 1.5% KCN for excitation (a) in the region of the vibrational phonon sidebands of the interconfigurational $4f \rightarrow 5d$ transitions and (b) in the region of the intraconfigurational $^7F_0 \rightarrow {}^5D_0$ transition. The CN^- related sites are labeled with numbers 1, ... , 7. The sites *a*, *d* already present in the absence of CN^- are labeled according to Ref. 19.

B. Sm^{2+}-CN^- complexes

1. Electronic transitions

In Fig. 4 emission spectra for a KCl sample doped with both Sm^{2+} and CN^- are shown. For excitation at around 637 nm in the region of the zero phonon line of the Sm^{2+} transition the emission spectrum looks at first sight just as the one found in samples without CN^-. It consists of several groups of sharp lines due to emission from the $^5D_0$ to the crystal-field-split ^7F_j states. In a more detailed picture (Fig. 5), however, a substructure of the individual $4f^6 \rightarrow 4f^6$ transitions, best seen and indicated with an arrow close to the strongest line within the $^5D_0 \rightarrow {}^7F_1$ transitions. This substructure is not observed in samples which have not been doped with CN^- molecules and already suggests the presence of CN^--perturbed Sm^{2+} sites. In Fig. 5 the excitation spectrum of the emission (probed at the indicated spectral position) is depicted, showing that the excitation both in the $^7F_0 \rightarrow {}^5D_0$ (indicated by the point) and in the interconfigurational $^7F_0 \rightarrow 5d$ transition is possible. Again, almost no differences to the isolated Sm^{2+} can be found.

In order to study the substructure within the $^5D_0 \rightarrow {}^7F_j$ transition we measured the combined excitation-emission spectra for the two different spectral regions of excitation energy. To allow for a reliable and easy comparison we first took special care to perform the thermal quenching before measurements identically for the samples with and without CN^- doping and second we depict in Fig. 6(b) the same spectral ranges as in Fig. 2. Several new sites (1–5) can be found which appear already for lower CN^- concentration and increase equally relative to the main isolated Sm^{2+} site *a* with increasing CN^- doping. For that reason we believe that they are unambiguously related to center complexes involving one CN^- molecular ion. Less certain are the sites (6, 7). Especially site 6 could have been missed in Fig. 2 due to the spectral vicinity to site *a*. After identification of the different $Sm^{2+} - CN^-$ sites also the spectral regions of the other $^5D_0 \leftrightarrow {}^7F_j$ emission transitions can be investigated by CEES to find the site-specific energies of the ^7F_j states. The spectral overlap of the excitation energies for different sites and less-resolved emission lines in certain wavelength regions makes a complete assignment impossible, and therefore only the unambiguously identified $^5D_0 \rightarrow {}^7F_j$ transition energies are listed in Table I. The differences in transition energies found are all of the order of 1 meV or even less.

Besides the narrow zero-phonon emission lines also the vibrational phonon sidebands observed most pronounced for the $^5D_0 \rightarrow {}^7F_0$ emission transitions (shown expanded in Fig. 5) can be studied under site-selective excitation and one finds that the shape and spectral shift do not depend on the excited site.

In a similar way the excitation energy can be changed into the range of the interconfigurational transition. The vibrational substructure (zero-phonon lines) on the low-energy side of the excitation spectrum is well suitable for our site-selective technique. The resulting contour plot is shown in Fig. 6(a). Again characteristic peaks for certain combinations of excitation and emission energies appear and can be assigned to the different Sm^{2+} sites by comparison with Fig. 6(b). This way the interaction effects for the $4f$-

TABLE I. Spectral positions in eV of various Sm^{2+} and Sm^{2+}-CN^- zero-phonon transitions for different sites. For the cases no value is given no unambiguous assignment was possible.

Host	Site *a*	Site *d*	Site 1	Site 2	Site 3	Site 4	Site 5	Site 6	Site 7
$^7F_0 \rightarrow 5d$	1.946	1.952	-	-	1.942	1.945	1.939	1.950	1.942
$^5D_0 \rightarrow {}^7F_0$	1.7984	1.7986	1.7987	1.7980	1.7980	1.7980	1.7978	1.7984	1.7984
$^5D_0 \rightarrow {}^7F_1$	1.7669	1.7662	1.7670	1.7668	1.7660	1.7658	1.7665	1.7664	1.7675
	1.7626	1.7650	-	1.7626	-	1.7622	1.7622	-	-
	1.7587	1.7577	-	1.7586	-	1.7579	1.7582	-	-
$^5D_0 \rightarrow {}^7F_2$	1.7063	1.7067	-	-	1.7066	-	1.7061	1.7059	-
	1.7020	1.7016	-	1.7021	-	1.7018	1.7015	-	-
	1.6969	1.6980	-	1.6967	-	1.6964	1.6965	-	-
	1.6915	1.6929	-	1.6915	-	1.6908	1.6909	-	-
$^5D_0 \rightarrow {}^7F_3$	1.6113	-	-	1.611	-	1.611	1.6108	-	-
	1.6111	-	-	1.6108	-	1.6108	1.6106	-	-
$^5D_0 \rightarrow {}^7F_4$	1.5132	-	-	1.5131	-	1.5128	1.5126	-	-
	1.5113	-	-	-	-	-	-	-	-
	1.5110	-	-	1.5109	1.5107	-	1.5102	-	-

and $5d$-type Sm^{2+} states with the CN^- can be compared. For the sites *a*, *d*, and 3–7 the corresponding peaks can easily be found (indicated by the lines) and the energy of the corresponding $5d$ state can be determined (included in Table I). The differences in transition energies are about 10 meV. For sites 1 and 2 an identification is not possible since the emission energy is hardly distinguishable from the strongly emitting site *a*.

While the spectral changes described so far are quite small, much more pronounced effects are found in the emission which appears as a background under excitation over the whole studied spectral range. As an example we show in the inset of Fig. 4 such a kind of spectra which consist of a very broad band with only very faint sharper features on top of it. The position for excitation ($\lambda = 690$ nm) was chosen in this case such that it does not coincide with any of the sharp spectral features of the spectra discussed above (Fig. 4). The emission band is strongly dependent in strength and spectral shape on the excitation position, suggesting a strong inhomogeneous broadening. Most notably, it shifts to lower energy as the excitation wavelength increases. Under CN^- concentration variation one finds that it is totally absent for samples not doped with CN^-. Under increase of CN^- concentration the emission increases superlinear in integrated intensity and shifts to lower energies as well. This behavior shown in the emission spectra (Fig. 4, inset) for two concentrations indicates that the Sm^{2+} energy levels are shifting towards lower energy as the average number of CN^- neighbors increases.

2. Vibrational luminescence

The question if and for which defect types *E*-*V* energy transfer takes place can easily be checked by measurement of the vibrational luminescence (VL). In Fig. 7 the VL spectrum under excitation at 690 nm is shown. The VL signal which consist of three main peaks is very weak—at least one order of magnitude weaker than for Yb^{2+}-$(CN^-)_n$ centers[10,4]—and could therefore only be detected reliably for our highest-doped sample (1.5% CN^-). By comparison with the VL spectra from other defect systems like Yb^{2+}-$(CN^-)_n$ and F_H (CN^-)[10,1] these peaks can be assigned to the vibrational transitions of regular unpaired CN^- defects with different isotopical compositions ($^{12}C^{14}N$, $^{13}C^{14}N$, $^{12}C^{15}N$). Obviously, an efficient vibrational (*V*-*V*) energy transfer from the initially excited CN^- molecules

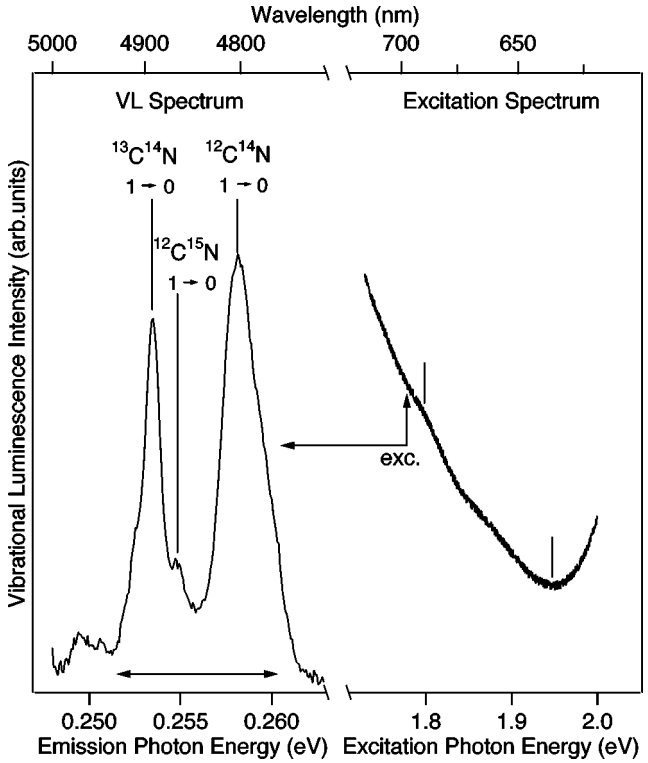

FIG. 7. Vibrational luminescence in $KCl:Sm^{2+} + 1.5\%$ KCN. Left: emission spectrum. The corresponding vibrational transitions are labeled. Right: excitation spectrum of VL. The spectral position of excitation and probing the emission are indicated by arrows. The spectral positions for which sharp feature would be expected are indicated with lines.

which have a Sm^{2+} neighbor to isolated CN^- molecules can take place similarly to what has been found for F_H (CN^-) centers[26] and is expected for a fairly high CN^- concentration. Only the weak peak around 0.250 eV could be a candidate for VL from Sm^{2+}-perturbed CN^-. For lower CN^- concentrations for which the *V-V* transfer should play a minor role the VL signal was too small to be spectrally resolved. By comparison of the integrated electronic and vibrational luminescence intensities the quantum efficiency of the *E-V* transfer can be estimated to be less than 1%.

In order to find out which types of Sm^{2+}-CN^- complexes are participating in the *E-V* transfer we measured the excitation spectrum of the VL. For the spectral range of the dye laser which was used the result is illustrated in Fig. 7 (right) and shows that the VL can be excited over a wide spectral range. No sharp excitation peaks appear, in obvious contrast to the spectrum for the electronic emission (shown in Fig. 5 and indicated in Fig. 7 by lines) of the simple Sm^{2+}-CN^- sites. Unfortunately, the spectral range we were able to study is not sufficient to cover the complete VL excitation spectrum. A measurement at 980 nm showed that even for this low excitation energy some weak VL signal is present. The VL intensity is somewhat higher in well-aged samples compared to the signal found after the sample has been quenched just before the measurements. This indicates that center aggregation is playing a role. However and in contrast to F_H (CN^-) and F_H (OH^-) centers, no method for a systematic pairing of the defect partners by controlled thermal annealing or light illumination could be found.

Under increasing temperature the VL signal decreases similarly to what has been seen for other systems. The main cause for this behavior is the increasing non-radiative decay within the vibrational CN^- excitation. Taking this well studied behavior of the isolated CN^- in KCl (Ref. 27) into account we found a constant or even slightly increasing *E-V* transfer efficiency up to $T=100$ K.

IV. SUMMARY AND DISCUSSION

The presented experimental data reveal many interesting features but also the complexity of the KCl:Sm^{2+}:CN^- system. To completely understand all aspects a more comprehensive study would be necessary similar to the one performed for KCl:Sm^{2+} by Ramponi and Wright.[19,25] This holds especially for the center formation processes, but it is beyond the scope of this report. We will concentrate in the following discussion on the questions raised above in Sec. I.

A. Energy levels and center structure

1. $(Sm^{2+})_n$ complexes

For the following discussion of the transition energies we will refer again to the schematic level diagrams in Figs. 1(a)– 1(c), although also other models have been proposed.[28]

The emission spectra we measured in the well-aged KCl:Sm^{2+} sample (see Fig. 3) strongly resemble the ones in NaBr, RbI, ... For that reason we conclude that in these aggregated $(Sm^{2+})_n$ center types the level *E* is also shifted below the $^5D_0$ state. In this interpretation, the observed groups $(1,\ldots,4)$ of emission bands indicated in Fig. 3 are assigned to the $E\rightarrow{}^7F_j$ $(j=1,\ldots,4)$ transitions. The sharp equidistant peaks on top of the bands can be identified as a vibrational substructure caused by coupling to a localized mode with a frequency ($\omega_{loc}\approx 11$ meV) considerably lower than for the mode (≈ 26 meV) which was found for isolated Sm^{2+} defects.[29] This indicates that the Sm^{2+} surrounding is strongly changed within these complexes compared to the isolated Sm^{2+}. The fine substructure within each peak is evidence for the presence of several complex center types.

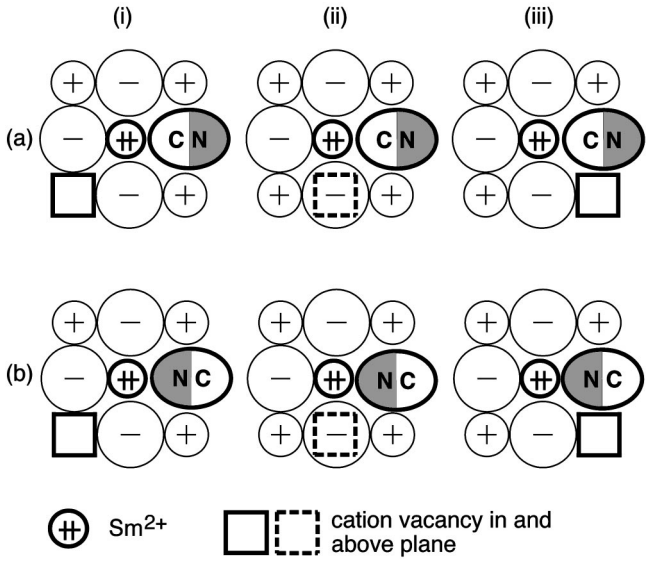

FIG. 8. Possible configurations of Sm^{2+}-CN^- complexes in KCl. For details see the text.

2. Sm^{2+}-CN^- centers

The different Sm^{2+}-CN^- sites observed in KCl:Sm^{2+} samples with low CN^- concentration and under excitation in the region of both the $^7F_0\rightarrow{}^5D_o$ and $^7F_0\rightarrow 5d$ absorption exhibit transitions almost identical in their spectral positions to the isolated Sm^{2+} defects. For that reason the energy level scheme in Fig. 1(a) is still applicable almost without modification and is repeated as a starting point $n=1$ in Fig. 1(c). The weak interaction of the $4f$ states to the surrounding which can directly be deduced for the electron coupling to phonons from the dominance of the zero-phonon emission transitions is further reflected in the vibrational sideband spectrum by the absence of any CN^--related localized mode.

Although our optical measurements are not suitable to identify directly the microscopic configuration of these centers, the number of different sites and the CN^- concentration dependence suggest that these are simple Sm^{2+}-CN^- complexes with a different arrangement and orientation of the CN^- relative to the Sm^{2+} and the required charge compensating cation vacancy: Assuming that the CN^- is in a $\langle 100\rangle$ neighborhood to the Sm^{2+}, the 12 possible $\langle 110\rangle$ positions of the vacancy can be classified into 3 groups (i), (ii), and (iii) with 4 equivalent arrangements. For each of the 3 groups 2 orientations (a,b) of the CN^- electric dipole are possible. The resulting six different configurations are shown in Fig. 8. This somewhat tentative assignment is supported by the fact that in Yb^{2+}-doped samples analogous configurations are observed.[10] The spectral changes for the Sm^{2+}-CN^- are very small, even smaller than the shifts found for certain

simple Sm^{2+} complexes.[19] Similar to the latter, the changes in energy observed for the $4f$ states are about 10 times smaller than for the lowest $5d$-type states. The shifts in both the $4f$ and $5d$ states can easily be accounted for by small differences in the crystal field which the Sm^{2+} ion experiences. This change can be caused by the weak permanent electric dipole moment of the CN^- and amplified by a displacement dipole due to an off-center CN^- position. Further interaction mechanisms like covalency effects and electron-exchange between the Sm^{2+}-CN^-, which become important for the Yb^{2+}-$(CN^-)_n$ centers, appear to be negligible.

3. Sm^{2+}-$(CN^-)_n$ clusters

In continuation of the arguments used for Sm^{2+} complexes we interpret the emission spectra obtained for higher CN^- concentrations and low-energy excitation (e.g., $\lambda = 690$ nm in Fig. 4). Their spectral shape is quite similar to that of the Sm^{2+} complexes although the substructures are much less pronounced. The increase of emission intensity with the CN^- doping level suggests that the responsible centers are Sm^{2+}-$(CN^-)_n$ clusters which involve more than one CN^- molecule. The redshift of the electronic emission under lowering of the excitation photon energy and increasing CN^- concentration can be explained in analogy to similar observations for Yb^{2+}-$(CN^-)_n$ and Eu^{2+}-$(CN^-)_n$. If we assume that the lowest $5d$-type level is shifted consecutively with increasing number n of involved CN^- molecules towards lower energies below the $^5D_0$ level, as indicated in Fig. 1(c), laser pumping at lower photon energies will result in excitation of centers with more CN^- incorporated into the complexes. Although an accurate energy level scheme as a function of n cannot be obtained from the measurements, it should be noted that the shifts of the $5d$ levels ($\Delta E > 100$ meV) are much more pronounced than expected from the purely additative behavior ($\Delta E = n \times 10$ meV) predicted for a mixed ligand case in the simple electrostatic crystal field theory. This indicates that a rearrangement of the ions within the complexes takes place, leading to stronger crystal field effects. The influence of covalency and electron exchange interaction neglected for the simple Sm^{2+}-CN^- complexes may become more appreciable.

The participation of more than one Sm^{2+} ion within these complexes cannot be excluded completely. The observation that the emission is still present after quenching suggests, however, that these complexes do not play a major role. Even if this possibility is neglected the Sm^{2+}-$(CN^-)_n$ complex configuration offers a large number of possible variations explaining the absence of a sharp emission substructure.

B. Energy transfer

The observed E-V energy transfer has a very low quantum efficiency and therefore the weak obtained VL signals do not allow a detailed study of certain aspects like accurate transfer rates and identification of the initially excited vibrational level. However, several clear statements can still be made.

(1) Simple Sm^{2+}-CN^- defects do not show E-V transfer as can be seen from the VL excitation spectrum. Only Sm^{2+}-$(CN^-)_n$ center complexes involving more than one CN^- molecule exhibit the transfer.

(2) These Sm^{2+}-$(CN^-)_n$ center complexes exhibit broad emission spectra and are characterized by $5d$-type levels which lie below the $4f$-type excited state Fig. 1(c). Their lowest $5d$ levels are the most likely origin for the transfer.

(3) The increase of VL signal for lower excitation energies suggests that the E-V transfer becomes more effective the more the $5d$ states are shifted to lower energies, i.e., the more CN^- are incorporated in the defect complexes.

Several theoretical models to account for the E-V energy transfer between electronic defects and molecular vibrations have been proposed and worked out mathematically. They can be divided roughly into two groups: first, the Förster-Dexter-(FD-) type transfer models which attribute the energy transfer to the interaction between transition dipoles or higher moments[30,31] and second, several models (like the ''supermolecule'' model, the cross over model, and the frequency-shifted CN^- oscillator model), which all assume an electronic vibrational coupling similar to the electron-phonon interaction.[32–34,13] While the latter ones are best suited for a strong coupling, the FD model can easily be applied also for weakly coupled systems and for interaction over longer distances, so that it is commonly used for a qualitative interpretation of the energy transfer between rare earth ions in numerous systems. In the FD model the E-V transfer rate W_{EV} from the lowest (Sm^{2+}) electronic excited state $(e,0,0)$ to an electronic ground state (g,m,μ) involving an excitation of m CN^- vibrations and μ phonon modes can be described for a dipole-dipole interaction by the following expression:[30]

$$W_{EV} = \frac{C}{R^6}\left\{\frac{d\langle\mu_{\mathrm{CN}}\rangle}{dq_{\mathrm{CN}}}\right\}^2_{q_{\mathrm{CN}}=q_0} |\langle\chi_m^{\mathrm{CN}}|q_{\mathrm{CN}}|\chi_0^{CN}\rangle|^2 \times \langle\mu_{\mathrm{Sm}}\rangle^2 \sum_{\mu} S_{\mu_g,0_e}\,\delta(E_{e,0,0}-E_{g,m,\mu}), \qquad (1)$$

with $\langle\mu_{\mathrm{Sm}}\rangle$ the electronic Sm^{2+} transition moment, χ_m^{CN} and q_{CN} the CN^- vibrational wave functions and coordinate, $S_{\mu_g,0_e}$ the Franck-Condon factor, and a constant C. The equation shows the characteristic $1/R^6$ dependence on the distance R between the energy donor and energy acceptor. Equation (1) can be interpreted more intuitively as the spectral overlap of the emission of the energy donor (3 factor) and the absorption of the acceptor (2 factor).[31] Within this model the absence of E-V transfer for the simple Sm^{2+}-CN^- complex can be accounted for by a lack of overlap between the sharp electronic and vibrational transitions. Moreover, it is expected and experimentally observed that for the weakly CN^- anharmonic oscillator the transition probability from the ground state to excited v states becomes drastically lower towards higher v numbers. This makes the E-V transfer less likely for higher energies and a large number of transferred vibrational quanta—similar to the energy gap law often found for nonradiative transitions. The conditions for the Sm^{2+}-$(CN^-)_n$ complexes are more favorable and the arguments from above can be used to explain the appearance of E-V transfer because these complexes show a broad luminescence (Fig. 4) with increasingly redshifted peak energies. The mentioned strong dependence of the vibrational absorption strength on Δv should favor an E-V transfer which involves electronic transitions into ground-state levels ^7F_j with higher energy and hence high j value, so that less energy has to be transferred.

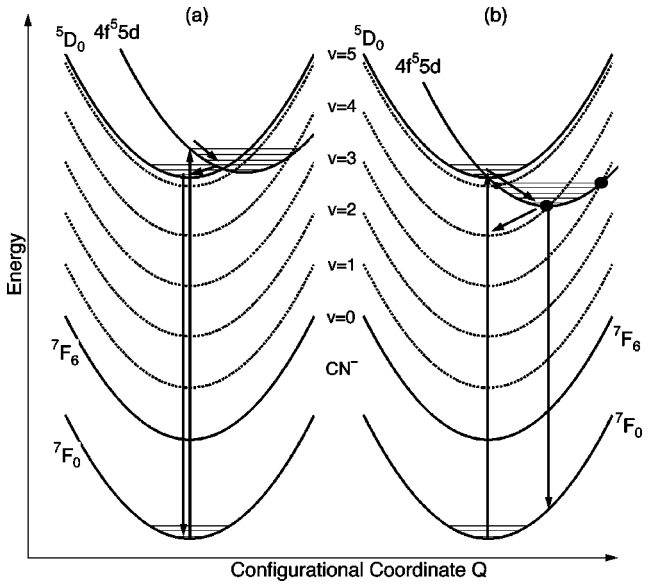

FIG. 9. Configurational coordinate representation of a simplified scheme of the Sm^{2+} electronic states (a) for isolated Sm^{2+} and simple Sm^{2+}-CN^- complexes and (b) for Sm^{2+}-$(CN^-)_n$, $n>1$. For the $^7F_6$ level vibrational CN^- energy levels are depicted as properly shifted additional curves. For details see the text.

While the influence of the electron-vibrational coupling on the E-V transfer which we intended to investigate is not explicitly included in the FD model, it plays a major role in all the other models mentioned above. These models and the electron vibrational coupling can best be visualized in the widely used configurational coordinate (CC) diagram in which the complete vibrational mode spectrum of the lattice with its coupling to the electronic defects is approximated by a single mode with one displacement coordinate Q and frequency ω. This kind of CC diagram has also been used by Fong[28] to explain the temperature dependence of the lifetime and spectral shape of the electronic luminescence of Sm^{2+} in KCl. Adapting the qualitative interpretation of the E-V transfer in $F_H(CN^-)$ centers by Rong and Luty[2] we can make a schematic model as shown in Fig. 9. The vibrational excitation levels are drawn as additional curves shifted successively upwards in energy relative to the Sm^{2+} levels by the CN^- vibrational energy (0.250 eV) for each additional v excitation. For simplicity, this is only done for the highest $(j=6)$ of the ^7F_j levels for which the most efficient E-V transfer is expected. Two situations are depicted: In Fig. 9(a) the weakly coupled $^5D_0$ state—represented by a potential curve barely shifted relative to the $^7F_0$ ground state—is the lowest-lying excited state as found for the simple Sm^{2+}-CN^- defect. In this case the excited electron relaxes fast into the $^5D_0$ level and no crossing point between the electronic and vibrationally excited levels can be reached at which a crossover between the potential curves could take place. This explains the absence of E-V energy transfer at least for the considered low temperatures. The observed small improvement of the transfer efficiency with increasing temperature can be explained by a thermally induced population of the $5d$ state.

In Fig. 9(b) the lowest-lying $5d$ state is lower in energy than the $^5D_0$ state. The $5d$ state exhibits a stronger coupling reflected in a stronger horizontal shift of its potential curve. In this case one finds several crossing points close to the potential minima at which an energy transfer is possible. This explains quite naturally the observation that for Sm^{2+}-$(CN^-)_n$ complexes with low-lying $5d$ states E-V transfer takes place. The exact mechanism of the crossover from one potential curve to the other depends on the adapted model. Unfortunately, within none of them can the absolute energy transfer rate be calculated; only relative efficiencies for the transfer channels into different CN^- vibrational states can be obtained always with similar results: At lowest temperatures the transfer at the lowest crossing point is most likely. In the depicted case this would be $v=4$.

In summary we have shown that the interaction and energy transfer between the Sm^{2+} and the CN^- molecules strongly depends on which electronic levels are involved and on how these are coupled to the lattice. Already these first results show that further investigations—similar to the extended studies on $F_H(CN^-)$—will shed more light on the nature of the electron-molecular interaction especially if the possibility to directly compare the behavior of $4f$- and $5d$-type states is further exploited.

ACKNOWLEDGMENTS

The author gratefully acknowledges discussions with Professor F. Luty and Dr. C. P. An in the early stages of this work. He thanks Dr. M. Yoshida for performing some of the CEES measurements and Professor W. von der Osten for reading and discussing the manuscript.

[1] Y. Yang and F. Luty, Phys. Rev. Lett. **51**, 419 (1983).
[2] F. Rong and F. Luty, Cryst. Lattice Defects Amorphous Mater. **18**, 1 (1989).
[3] V. Dierolf, J. Hoidis, D. Samiec, and W. von der Osten, J. Lumin. **76&77**, 581 (1998).
[4] M. Müller, J. F. Fabris, A. C. Hernandes, and M. Siu-Li, J. Lumin. **59**, 289 (1994).
[5] E. Gustin, M. Leblans, A. Bouwen, and D. Schoemaker, Phys. Rev. B **54**, 6963 (1996).
[6] D. Samiec, H. Stolz, and W. von der Osten, Phys. Rev. B **53**, 8811 (1996).
[7] A. Naber, in *Defects in Insulating Materials, Proceedings of ICDIM92)*, edited by O. Kanert and J.-M. Spaeth (World Scientific, Singapore, 1993), p. 545.
[8] H. Söthe, J.-M. Spaeth, and F. Luty, J. Phys. Condens. Matter. **5**, 1957 (1993).
[9] V. Dierolf and F. Luty, Phys. Rev. B **54**, 6952 (1996).
[10] V. Dierolf, C. P. An, and F. Luty (unpublished).
[11] F. Luty and V. Dierolf, in *Defects in Insulating Materials, Proceedings of ICDIM92* (Ref. 7), p. 17.
[12] G. Halama, K. T. Tsen, S. H. Lin, and J. B. Page, Phys. Rev. B **44**, 2040 (1991).
[13] S. Pilzer and W. B. Fowler, in Proceedings of ICDIM96, edited by G. E. Matthews and R. T. Williams [Mater. Sci. Forum

239-241, 473 (1997)].
[14] P. W. Gash, Phys. Rev. B **35**, 774 (1987).
[15] J. West, K. T. Tsen, and S. H. Lin, Mod. Phys. Lett. **9**, 1759 (1995).
[16] P. W. Gash, in Proceedings of ICDIM96, edited by G. E. Matthews and R. T. Williams [Mater. Sci. Forum **239-241**, 373 (1997)].
[17] J. O. Rubio, J. Phys. Chem. Solids **52**, 101 (1991).
[18] F. M. M. Yasuoka, J. C. Castro, and L. A. O. Nunes, Phys. Rev. B **43**, 9295 (1991).
[19] A. J. Ramponi and J. C. Wright, Phys. Rev. B **31**, 3965 (1985).
[20] W. E. Bron and W. R. Heller, Phys. Rev. **136**, A1433 (1964).
[21] M. Guzzi and G. Baldini, J. Lumin. **6**, 270 (1973).
[22] W. Kaiser, C. G. W. Garrett, and D. L. Wood, Phys. Rev. **123**, 176 (1961).
[23] G. Baldini and M. Guzzi, Phys. Status Solidi **30**, 601 (1968).
[24] E. Mulazzi, G. F. Nardelli, and N. Terzi, Phys. Rev. **172**, 847 (1968).
[25] A. J. Ramponi and J. C. Wright, Phys. Rev. B **35**, 2413 (1987).
[26] V. Dierolf and F. Luty, Rev. Solid State Sci. **4**, 479 (1990).
[27] K. P. Koch, Y. Yang, and F. Luty, Phys. Rev. B **29**, 5840 (1984).
[28] F. K. Fong, in *Theory of Molecular Relaxation, Application in Chemistry and Biology* (Wiley, New York, 1975).
[29] M. Wagner and W. E. Bron, Phys. Rev. **139**, A223 (1965).
[30] G. Halama, K. T. Tsen, S. H. Lin, F. Luty, and J. B. Page, Phys. Rev. B **39**, 13457 (1989).
[31] W. B. Fowler (private communication).
[32] G. Halama, S. H. Lin, K. T. Tsen, F. Luty, and J. B. Page, Phys. Rev. B **41**, 3136 (1990).
[33] E. Gustin, M. Leblans, A. Bouwen, and D. Schoemaker, Phys. Rev. B **54**, 6977 (1996).
[34] A. Naber, Ph.D. thesis, Westfälische Wilhelms-Universität Münster, 1993.